# Searching for Exoplanets in the Hertzsprung Gap: An Eccentric Hot Jupiter Orbiting the Subgiant HD 185269<sup>1</sup>

John Asher Johnson<sup>2</sup>, Geoffrey W. Marcy<sup>2</sup>, Debra A. Fischer<sup>3</sup>, Gregory W. Henry<sup>4</sup>, Jason T. Wright<sup>2</sup>, Howard Isaacson<sup>3</sup>, Chris McCarthy<sup>3</sup>

johnjohn@astron.berkeley.edu

# ABSTRACT

We report the detection of a Jupiter–mass planet in a 6.838 d orbit around the 1.28  $M_{\odot}$  subgiant HD 185269. The eccentricity of HD 185269b (e=0.30) is unusually large compared to other planets within 0.1 AU of their stars. Photometric observations demonstrate that the star is constant to  $\pm 0.0001$  mag on the radial velocity period, strengthening our interpretation of a planetary companion. This planet was detected as part of our radial velocity survey of evolved stars located on the subgiant branch of the H–R diagram—also known as the Hertzsprung Gap. These stars, which have masses between 1.2 and 2.5  $M_{\odot}$ , play an important role in the investigation of the frequency of extrasolar planets as a function of stellar mass.

Subject headings: techniques: radial velocities—planetary systems: formation—stars: individual (HD 189269)

# 1. Introduction

The assemblage of  $\sim 185$  known extrasolar planets<sup>5</sup> has revealed important relationships between the physical characteristics of stars and the likelihood that they harbor planets (Udry et al. 2003; Butler et al. 2006). One example is the strong correlation between planet

<sup>&</sup>lt;sup>1</sup>Based on observations obtained at the Lick Observatory, which is operated by the University of California

<sup>&</sup>lt;sup>2</sup>Department of Astronomy, University of California, Mail Code 3411, Berkeley, CA 94720

<sup>&</sup>lt;sup>3</sup>Department of Physics & Astronomy, San Francisco State University, San Francisco, CA 94132

<sup>&</sup>lt;sup>4</sup>Center of Excellence in Information Systems, Tennessee State University, 3500 John A. Merritt Blvd., Box 9501, Nashville, TN 37209

<sup>&</sup>lt;sup>5</sup>For the updated catalog of extrasolar planet and their parameters see http://exoplanets.org.

occurrence and stellar metallicity (Gonzalez 1997; Santos et al. 2004; Fischer & Valenti 2005). The planet-metallicity relationship can be understood in the context of the core accretion model of planet formation, in which Jovian planets begin as large rocky cores that then accrete gas from their surrounding protoplanetary disks once they exceed a critical core mass (e.g. Pollack et al. 1996). The growth of these embryonic cores is enhanced by increasing the surface density of solid particles in the disk, which is related to the metallicity of the star/disk system (Alibert et al. 2005; Ida & Lin 2005a).

The growth rate of rocky cores in protoplanetary disks is also related to the total disk mass. Assuming that the disk mass increases with the mass of the central star, the planet occurrence rate should therefore also correlate with stellar mass. Laughlin et al. (2004) showed that the lower surface densities of M dwarf protoplanetary disks impede the growth of Jupiter–mass planets. The relationship between stellar mass and planet occurrence was studied in further detail by Ida & Lin (2005b) for a larger range of stellar masses. Based on their Monte Carlo simulations, they predict a positive correlation between the number of detectable planets and stellar mass up to about 1  $M_{\odot}$ . However, there is some debate about whether surface density of solid material in protoplanetary disks is proportional to the mass of the central star. By assuming that the initial conditions of the disk are independent from the mass of star, Kornet et al. (2006) find that the occurrence rate of planets is inversely related to stellar mass.

The prediction that low–mass stars should have a lower frequency of Jovian planets is in accordance with observations; only one M dwarf, GL 876, is known to harbor Jupiter–mass planets (Marcy et al. 2001). From their survey of 90 M dwarfs, Endl et al. (2006) estimate that less than 1.27% of such low–mass stars harbor Jovian–mass planets within 1 AU. This finding cannot be attributed to an observational bias since the amplitude of a star's reflex motion scales as  $K \propto M_{star}^{-2./3}$ .

Laws et al. (2003) studied the planet occurrence rate in light of the current observational data using the larger set of FGK stars surveyed as part of the California & Carnegie Planet Search (CCPS, the full, updated target list can be found in Wright et al. (2004))). They found evidence that the planet rate decreases for lower stellar masses and peaks near 1.0  $M_{\odot}$ . However, the planet rate is poorly constrained for stellar masses greater than about 1.2  $M_{\odot}$  due to the small number of intermediate—mass stars (1.3  $\lesssim M_{star} \lesssim 3~M_{\odot}$ ) in the CCPS sample. This dearth of massive stars is due to an observational bias since main—sequence stars with spectral types earlier than F8 tend to be fast rotators (do Nascimento et al. 2003), have fewer spectral lines, and display a large amount of chromospheric activity (Saar et al. 1998). These features result in a decrease in the radial velocity precision attainable from the spectra of main—sequence stars more massive than  $\sim 1.2~M_{\odot}$  (Galland et al. 2005). Thus,

early-type dwarfs are not typically monitored as part of most radial velocity surveys.

One method to circumvent these difficulties is to observe intermediate—mass stars after they evolve into the region of the H–R diagram between the main—sequence and red giant branch—also known as the Hertzsprung Gap (HG). After stars have expended their core hydrogen fuel sources their radii expand, their photospheres cool, and convection sets in below their photospheres. Convective motion and stellar rotation drive magnetic fields that couple with an expanding stellar wind and act as a rotational brake (Gray & Nagar 1985; Schrijver & Pols 1993; do Nascimento et al. 2000). The cooler atmospheres and slower rotational velocities of evolved stars lead to an increased number of narrow absorption lines in their spectra, making HG stars better suited for precise radial velocity measurements than their main—sequence progenitors.

We are conducting a radial velocity survey of 159 HG stars to search for planets orbiting intermediate—mass stars. We describe the selection criteria of our sample of stars in § 2. We present here the first planet detection from our sample of HG stars: an eccentric hot jupiter orbiting the 1.28  $M_{\odot}$  subgiant, HD 185269. The properties of the host star are presented in § 3, and we describe our observations and orbital solution in § 4. We present the results of our photometric monitoring in § 5 and conclude with a discussion in § 6.

# 2. Sample

We have selected 159 HG stars based on the criteria  $0.5 < M_V < 3.5$ , 0.55 < B-V < 1.0, and  $V \lesssim 7.6$ , as listed in the Hipparcos Catalog (ESA 1997). Additionally, we selected only stars lying more than 1 mag above the mean Hipparcos main–sequence, as defined by Wright (2004). We chose the red cutoff to avoid red giants, which are known to exhibit excess velocity jitter (Frink et al. 2001; Hekker et al. 2006). The lower  $M_V$  restriction avoids Cepheid variables, and the upper limit excludes stars with masses less than  $1.2 M_{\odot}$ . We avoided stars in the clump region of the H–R diagram (B-V>0.8 and  $M_V<2.0$ ) in order to avoid the mass ambiguity stemming from the closely–spaced, overlapping isochrones between low–mass horizontal branch stars and high–mass stars on their first ascent to the giant branch.

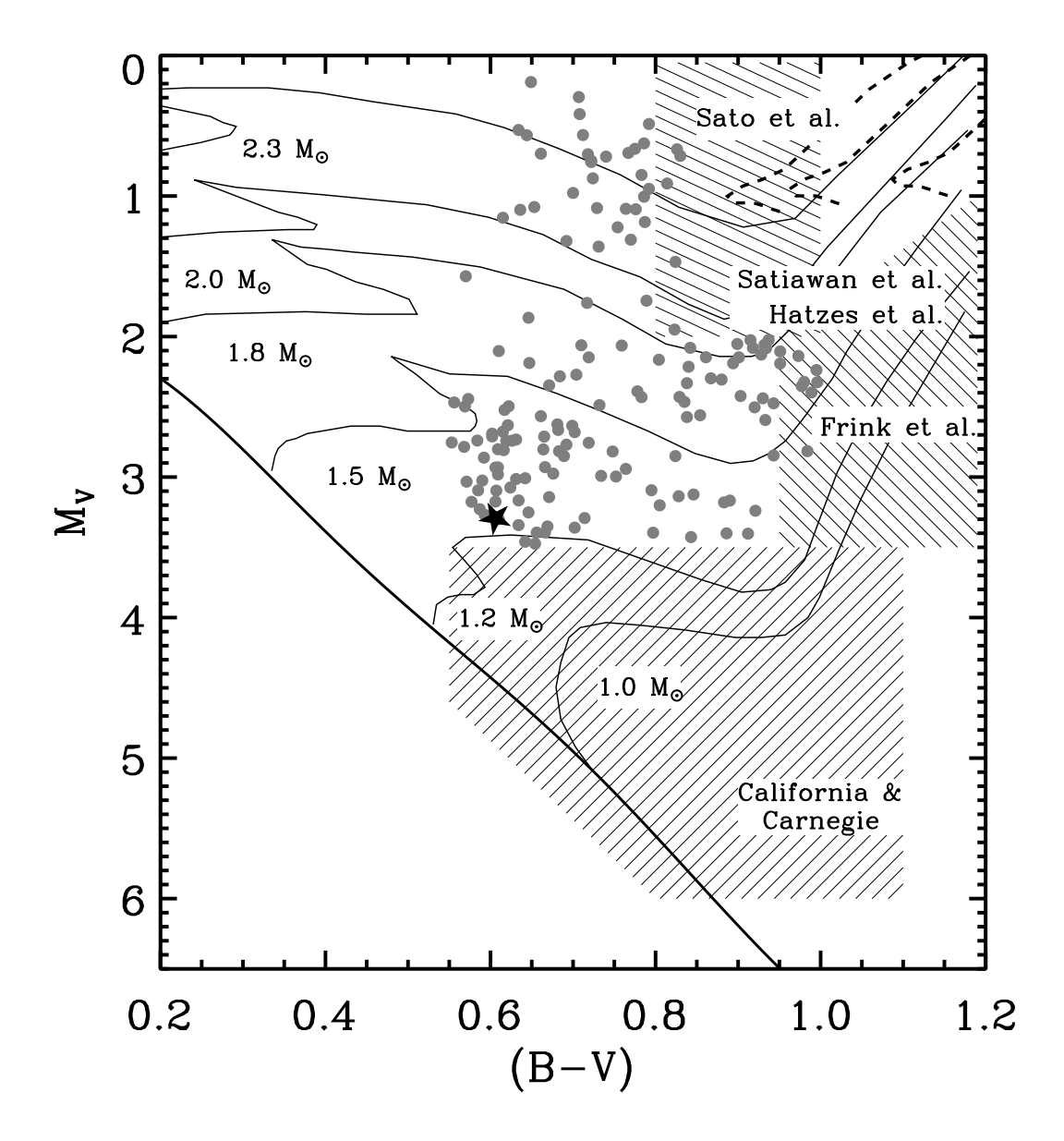


Fig. 1.— Our sample of Hertzsprung Gap stars (filled circles) with respect to the mean Hipparcos main–sequence (thick line) and the theoretical mass tracks of Girardi et al. (2002) for [Fe/H] = 0.0. The mass tracks for Solar–mass stars on the horizontal branch with  $[Fe/H] = \{-0.7, -0.4, 0.0\}$  (from left to right) are shown as dashed lines in the upper right portion of the figure. The overlapping mass tracks in this region of the H–R diagram leads to ambiguious mass estimates. The filled star shows the position of HD 185269. The hashed regions show the approximate ranges of the samples of other planet search programs.

The H–R diagram of our full sample is illustrated in Figure 1, along with the mass tracks of Girardi et al. (2002). The mass range of our sample is  $1.2 < M_* \lesssim 2.5 M_{\odot}$ , with a mean of  $1.5 M_{\odot}$ . We are observing 115 of the brightest and northernmost of these stars at Lick Observatory and the remaining 44 at Keck Observatory. Figure 1 also shows the approximate search domains of other programs containing evolved, intermediate—mass stars. These surveys include searches for planets around clump giants (Sato et al. 2003; Setiawan et al. 2003), red giants (Frink et al. 2002; Hatzes et al. 2005) and the subgiants included in the CCPS. As evidenced from Figure 1, HG stars occupy a unique and unexplored region in the H–R diagram.

## 3. Properties of HD 185269

HD 185269 (=HIP 96507) is a G0IV subgiant with V=6.67, B-V=0.606, a parallax-based distance of 47.6 pc, and an absolute magnitude  $M_V=3.29$  (ESA 1997). Its position in the H–R diagram in relation to other stars in our sample is shown in Figure 1. HD 185269 lies 1.1 mag above the mean Hipparcos main–sequence of stars in the solar neighborhood (Wright 2004), confirming its subgiant classification. This star is chromospherically–quiet with S=0.14 and  $R'_{HK}=-5.14$ , from which we estimate a 23 d rotation period. We used the LTE spectral synthesis described by Valenti & Fischer (2005) to calculate  $T_{eff}=5980$  K, [Fe/H]=+0.11,  $\log g=3.94$  and  $V_{rot}\sin i=6.1$  km s<sup>-1</sup>. We interpolated the star's color, absolute magnitude and metallicity onto the stellar model grids of Girardi et al. (2002) using the Bayesian methodology detailed by Pont & Eyer (2004). Our interpolation yields an estimated stellar mass  $M_*=1.28\pm0.1~M_{\odot}$ , radius  $R_*=1.88\pm0.07~R_{\odot}$ ; in agreement with  $M_*=1.31~M_{\odot}$  and  $R_*=1.74~R_{\odot}$  estimated by Allende Prieto & Lambert (1999). All of the stellar properties are summarized in Table 1.

#### 4. Observations and Orbit

We began observing HD 185269 in 2004 May at Lick Observatory using the 0.6 m Coude Auxiliary Telescope (CAT) and the 3 m Shane telescope. Both telescopes feed the Hamilton echelle spectrograph, thus no offset correction is needed for the velocities. We measured radial velocities from the high–resolution ( $\lambda/\delta\lambda=50,000$ ) spectral observations using the Butler et al. (1996) iodine cell method. Traditionally, this method requires an additional reference observation, or template, made without the iodine cell. These template observations require higher signal and resolution than normal radial velocity observations, which leads to increased exposure times. Given our large target list and the small aperture of the CAT, obtaining

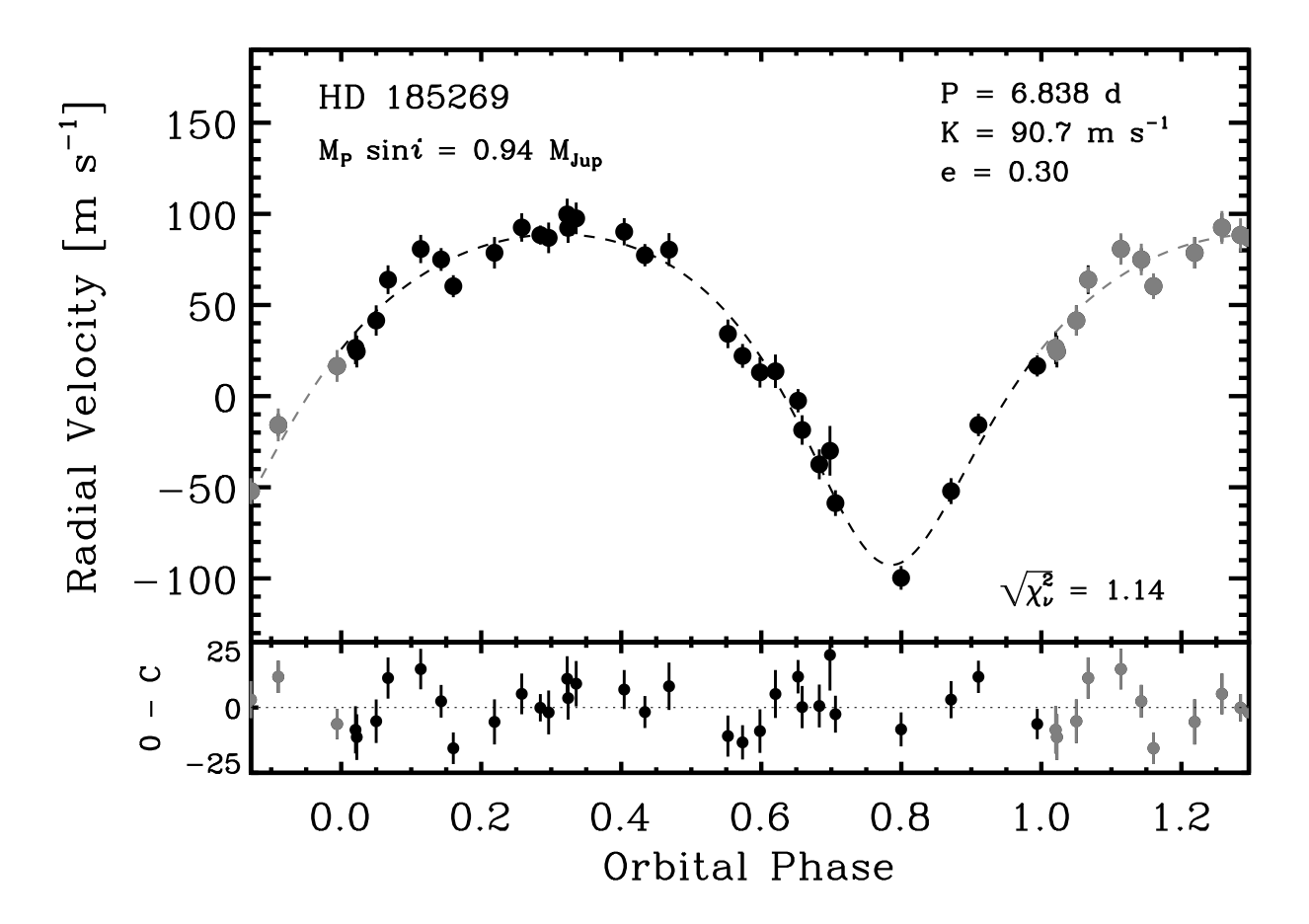


Fig. 2.— Phased radial velocity measurements of HD 185269. The dashed line shows the best–fit orbital solution. The bottom panel shows the phased residuals of the fit, which have  $RMS = 10.1 \text{ m s}^{-1}$ .

an observed template for each star would represent a prohibitive cost in observing time. We instead analyze the initial observations of all our targets using synthetic (or "morphed") templates, following the method described by Johnson et al. (2006). Stars showing excess RMS scatter are reanalyzed using a high–quality observed template, obtained with the 3 m Shane telescope, to achieve improved long–term velocity precision.

The first five observations of HD 185269 spanned 1 yr and had an RMS scatter of  $53 \text{ m s}^{-1}$ , prompting us to initiate follow-up observations with an increased sampling rate to search for a short-period signal. Our radial velocity measurements are listed in Table 2 along with the Julian dates and internal measurement uncertainties. A periodogram analysis of the velocities reveals a 6.838 periodicity with a false alarm probability < 0.001%. To search for a full orbital solution, we augmented our measurement uncertainties with a jitter estimate of  $5.0 \text{ m s}^{-1}$ , based on the star's chromospheric activity index, absolute magnitude

and color (Saar et al. 1998; Wright 2005). The best-fit Keplerian orbital solution yields an orbital period P=6.838 d, velocity semi-amplitude K=91 m s<sup>-1</sup> and eccentricity  $e=0.30\pm0.04$ . Using our stellar mass estimate of  $1.28~M_{\odot}$ , we derive  $M_P \sin i = 0.94~M_{\rm Jup}$  and a=0.077 AU. Figure 2 shows our velocities and orbital solution phased with the 6.838 d period. The full orbital solution and parameter uncertainties are listed in Table 3.

We estimate the parameter uncertainties using a Monte Carlo method. For each of 100 trials the best–fit Keplerian is subtracted from the measured velocities. The residuals are then scrambled and added back to the original measurements, and a new set of orbital parameters is obtained. The standard deviations of the parameters derived from all trials are adopted as the  $1\sigma$  uncertainties listed in Table 3.

#### 5. Photometric Observations

Queloz et al. (2001) and Paulson et al. (2004) have shown that active regions such as spots and plages on the photospheres of solar-type stars can cause low-amplitude, radial velocity variations (jitter) by distorting the stellar line profiles as the spots are carried across the stellar disk by rotation. If a large active region exists for several stellar rotations (not an unusual circumstance for stars younger and more active than the Sun), then periodic rotational modulation of the spectral line profiles can mimic the presence of a planetary companion. Therefore, precision photometric measurements can be an important complement to Doppler observations. For radial velocity variations caused by surface magnetic activity, the star will exhibit low-level photometric variability (e.g., Henry et al. 1995) on the radial velocity period. If the radial velocity variability is the result of true reflex motion caused by a planetary companion in orbit around the star, the star in general will not show photometric variability on the radial velocity period (e.g., Henry et al. 2000a). Photometric observations of planetary-candidate stars can also detect transits of planetary companions with inclinations near 90° and so allow the determination of a planet's true mass, radius, density, and composition (e.g., Henry et al. 2000b; Sato et al. 2005; Bouchy et al. 2005).

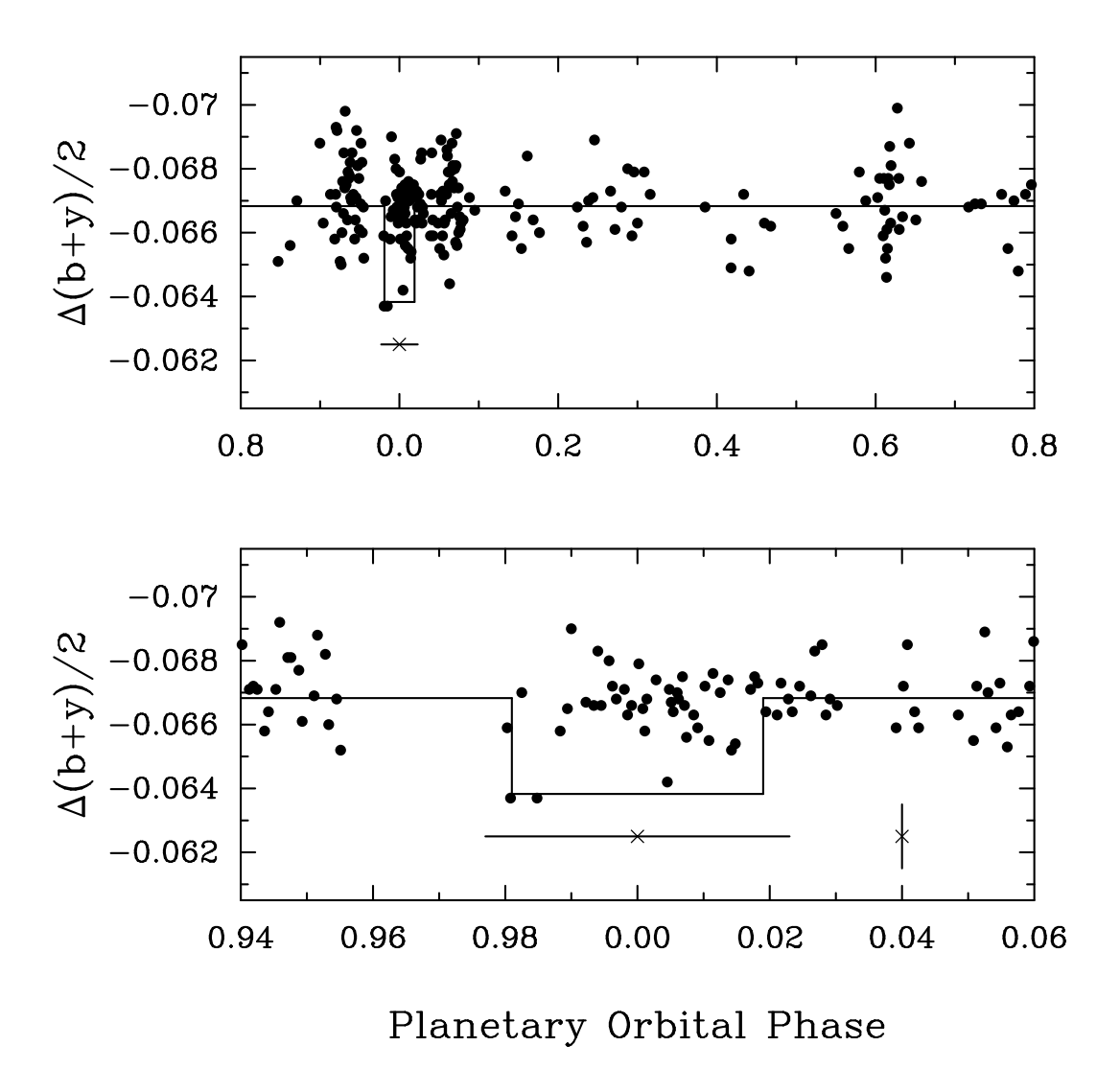


Fig. 3.— Strömgren (b+y)/2 photometric observations of HD 185269 acquired with the T11 0.8 m APT at Fairborn Observatory. The observations have been phased to the orbital period of the planet and an estimated time of mid transit. (Top) There is no evidence for any periodicity in the observations between 1 and 100 days. In particular, the star is constant on the radial velocity period to a limit of 0.0001 mag or so, supporting the planetary interpretation of the radial velocity variations. (Bottom) The photometric observations around the predicted time of transit replotted with an expanded scale on the abscissa. The predicted transit depth of only 0.003 mag is shown for an assumed planetary radius of 1  $R_{Jup}$ ; such transits are ruled out by the observations.

We observed HD 185269 with the T11 0.8 m automatic photometric telescope (APT) at Fairborn Observatory during May and June of 2006, obtaining a total of 207 brightness measurements. The T11 APT is equipped with a two-channel precision photometer employing two EMI 9124QB bi-alkali photomultiplier tubes to make simultaneous measurements in the Strömgren b and y passbands. The APT measures the difference in brightness between a program star and a nearby constant comparison star or stars with a typical precision of 0.0015 mag for bright stars (V < 8.0). For HD 185269, we used the two comparison stars  $HD 184151 \ (V = 6.87, B - V = 0.46, F5 \ V)$  and  $HD 184381 \ (V = 6.70, B - V = 0.45,$ F5 V). Differential magnitudes between the two comparison stars showed them both to be constant to 0.0012 mag or better on a night-to-night timescale. We created Strömgren b and y differential magnitudes of HD 185269 with respect to the average of the two comparison stars to improve our photometric precision. The differential magnitudes were reduced with nightly extinction coefficients and transformed to the Strömgren system with yearly mean transformation coefficients. To improve precision still further, we combined the separate band y differential magnitudes into a single (b+y)/2 pass band. Additional information on the telescope, photometer, observing procedures, and data reduction techniques employed with the T11 APT can be found in Henry (1999) and Eaton et al. (2003).

The 207 combined (b+y)/2 differential magnitudes of HD 185269 are plotted in the top panel of Figure 3. The observations are phased with the planetary orbital period and the time of mid transit given in Table 3. The standard deviation of the observations from the mean brightness level is 0.0011 mag, suggesting that HD 185269 as well as its comparison stars are all highly constant. Period analysis does not reveal any periodicity between 0.03 and 100 days. A least-squares sine fit of the observations phased to the radial velocity period gives a semi-amplitude of 0.00015  $\pm$  0.00012 mag. This very low limit to possible photometric variability supports planetary-reflex motion as the cause of the radial velocity variations.

In the bottom panel of Figure 3, the observations near phase 0.0 are replotted with an expanded scale on the abscissa. The solid curve in each of the two panels approximates the predicted transit light curve assuming a planetary orbital inclination of 90° (central transits). The out-of-transit light level corresponds to the mean brightness of the observations. The predicted transit duration is calculated from the orbital elements, while the predicted transit depth of 0.003 mag is derived from the stellar radius of 1.88  $R_{\odot}$  from Table 1 and an assumed planetary radius of 1.0  $R_{Jup}$ . Thus, any transits of the planet across the subgiant star are expected to be very shallow, as was the case with the transits of HD 149026 (Sato et al. 2005). The horizontal bar below the predicted transit window represents the approximate uncertainty in the time of mid transit, computed from the orbital elements. The vertical error bar to the right of the transit window corresponds to the  $\pm$  0.0011 mag measurement

uncertainties for a single observation. The geometric probability of transits in this system is  $\sim 12\%$ , computed from the orbital elements in Table 3 and equation 1 of Seagroves et al. (2003). Although the uncertainty in the time of mid transit is slightly larger than the predicted duration of any transits, the observations nonetheless rule out the existence of transits except perhaps for short events occurring around phase 0.97. In the absence of transits, the orbital inclination must be less than  $\sim 83^{\circ}$ .

## 6. Summary and Discussion

We are monitoring the radial velocities of a sample of 159 intermediate—mass Hertzsprung Gap (HG) stars in order to study the relationship between stellar mass and planet occurrence rate. We present the detection of a 0.94  $M_{\rm Jup}$  planet in an eccentric, 6.838 d orbit around the 1.28  $M_{\odot}$  subgiant HD 185269.

Compared to other planets with orbital separations a < 0.1 AU (also known as "hot jupiters"), HD 185269b has an unusually large eccentricity. Figure 4 shows the distribution of eccentricities for the 33 planets having a < 0.1 AU (Butler et al. 2006). With e = 0.30, HD 185269 b stands out from the distribution as one of only three hot jupiters with eccentricities in excess of 0.2. The other two planets are HD 162020 b (e = 0.277; Udry et al. 2002) and HD 118203 b (e = 0.309; da Silva et al. 2006).

The origin of eccentricities amongst single exoplanets is not well understood, but the gravitational influence of additional companions can drive the eccentricities of planets in multicomponent systems. An as–yet undetected second planet is likely the cause of the large eccentricity of HD 118203b—da Silva et al. (2006) report a linear trend with a 49.7 m s<sup>-1</sup> yr<sup>-1</sup> slope. However, we do not see evidence of a linear trend in our observations of HD 185269, nor significant periodicities in the Keplerian fit residuals. We are continuing to monitor this star at Keck and Lick Observatories to search for additional low–mass companions.

It is thought that the nearly circular orbits of most hot jupiters is a result of tidal circularization. This leaves open the possibility that the tidal circularization timescale at the orbital distance of HD 185269b is longer than the age of the star. Indeed, theoretical predictions of the circularization timescale have a strong dependence with semi-major axis, typically  $t_{circ} \propto a^{13/3}$  (Terquem et al. 1998). Eight of the 10 planets with a > 0.055 AU have eccentricities greater than 0.1, which may indicate that the timescale for tidal circularization at distances beyond  $\sim 0.055$  AU is longer than the age of most FGK stars. The detection of additional hot jupiters by programs such as the N2K Consortium (Fischer et al. 2005) will help shed light on the relationship between the eccentricity and orbital separation of

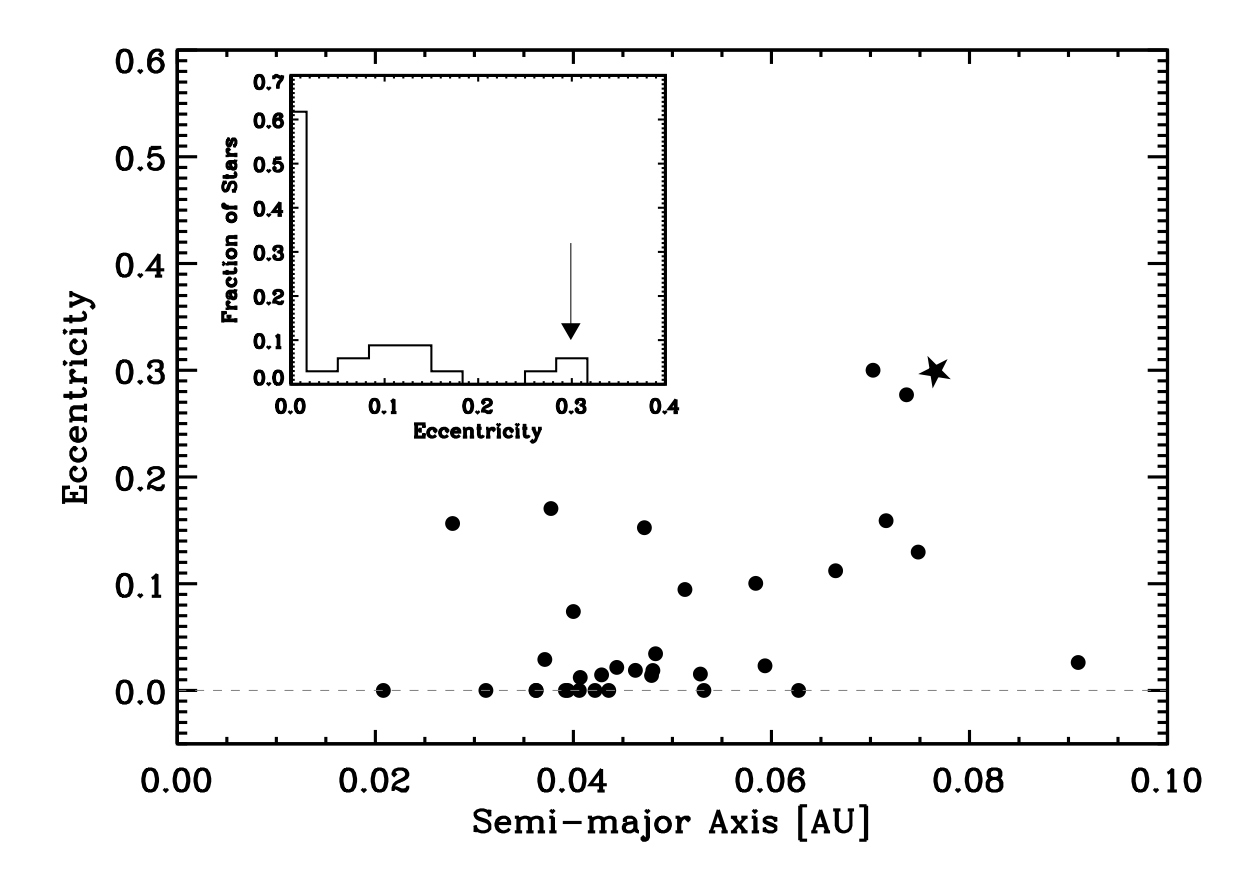


Fig. 4.— The eccentricity-period distribution of hot jupiters listed in Butler et al. (2006). HD 185269 is shown as a filled pentagram. The inset shows the histogram of eccentricities for the same sample of stars. The arrow denotes the position of HD 185269.

# short–period planets.

Other searches for planets around intermediate—mass stars have so far focused on the red giant branch (Frink et al. 2002; Hatzes et al. 2005) and clump regions of the H–R diagram (Sato et al. 2003; Setiawan et al. 2003). These programs have to date discovered a total of 6 sub-stellar objects orbiting giant stars, proving that planets do form and can be detected around evolved stars more massive than  $\sim 1.5 M_{\odot}$ . However, stars in the clump and red giant branches follow closely—spaced and often overlapping evolutionary tracks, making precise stellar mass estimations from isochrone interpolation difficult (see Figure 1). By contrast, HG stars have mass tracks that are nearly parallel and widely—spaced in  $M_V$ , enabling precise mass determinations. HG stars also exhibit lower velocity jitter and have smaller radii than red giants (Frink et al. 2001; Hekker et al. 2006), which enables the detection of a wider

range of planet masses and orbital separations. We will present the stellar characteristics and velocity behavior of our sample in a forthcoming paper.

We extend our gratitude to the many CAT observers who have helped with this project, including Shannon Patel, Julia Kregenow, Karin Sandstrom, Katie Peek and Bernie Walp. Special thanks to Conor Laver and Franck Marchis for lending a portion of their 3m time to observe this star before it set in 2005. We also gratefully acknowledge the efforts and dedication of the Lick Observatory staff. We appreciate funding from NASA grant NNG05GK92G (to GWM) for supporting this research. DAF is a Cottrell Science Scholar of Research Corporation and acknowledges support from NASA Grant NNG05G164G that made this work possible. GWH acknowledges support from NASA grant NCC5-511 and NSF grant HRD-9706268.

# REFERENCES

- Alibert, Y., Mordasini, C., Benz, W., & Winisdoerffer, C. 2005, A&A, 434, 343
- Allende Prieto, C. & Lambert, D. L. 1999, A&A, 352, 555
- Bouchy, F., Udry, S., Mayor, M., Moutou, C., Pont, F., Iribarne, N., da Silva, R., Ilovaisky, S., Queloz, D., Santos, N. C., Ségransan, D., & Zucker, S. 2005, A&A, 444, L15
- Butler, R. P., Marcy, G. W., Williams, E., McCarthy, C., Dosanjh, P., & Vogt, S. S. 1996, PASP, 108, 500
- Butler, R. P., Wright, J. T., Marcy, G. W., Fischer, D. A., Vogt, S. S., Tinney, C. G., Jones, H. R. A., Carter, B. D., Johnson, J. A., McCarthy, C., Munoz, M., & Penny, A. J. 2006, ApJ, submitted
- da Silva, R., Udry, S., Bouchy, F., Mayor, M., Moutou, C., Pont, F., Queloz, D., Santos, N. C., Ségransan, D., & Zucker, S. 2006, A&A, 446, 717
- do Nascimento, J. D., Canto Martins, B. L., Melo, C. H. F., Porto de Mello, G., & De Medeiros, J. R. 2003, A&A, 405, 723
- do Nascimento, J. D., Charbonnel, C., Lèbre, A., de Laverny, P., & De Medeiros, J. R. 2000, A&A, 357, 931
- Eaton, J. A., Henry, G. W., & Fekel, F. C. 2003, The Future of Small Telescopes In The New Millennium. Volume II The Telescopes We Use, 189

- Endl, M., Cochran, W. D., Kuerster, M., Paulson, D. B., Wittenmyer, R. A., MacQueen, P. J., & Tull, R. G. 2006, ArXiv Astrophysics e-prints
- ESA, . 1997, VizieR Online Data Catalog, 1239, 0
- Fischer, D. A., Laughlin, G., Butler, P., Marcy, G., Johnson, J., Henry, G., Valenti, J., Vogt, S., Ammons, M., Robinson, S., Spear, G., Strader, J., Driscoll, P., Fuller, A., Johnson, T., Manrao, E., McCarthy, C., Muñoz, M., Tah, K. L., Wright, J., Ida, S., Sato, B., Toyota, E., & Minniti, D. 2005, ApJ, 620, 481
- Fischer, D. A. & Valenti, J. 2005, ApJ, 622, 1102
- Frink, S., Mitchell, D. S., Quirrenbach, A., Fischer, D. A., Marcy, G. W., & Butler, R. P. 2002, ApJ, 576, 478
- Frink, S., Quirrenbach, A., Fischer, D., Röser, S., & Schilbach, E. 2001, PASP, 113, 173
- Galland, F., Lagrange, A.-M., Udry, S., Chelli, A., Pepe, F., Queloz, D., Beuzit, J.-L., & Mayor, M. 2005, A&A, 443, 337
- Girardi, L., Bertelli, G., Bressan, A., Chiosi, C., Groenewegen, M. A. T., Marigo, P., Salasnich, B., & Weiss, A. 2002, A&A, 391, 195
- Gonzalez, G. 1997, MNRAS, 285, 403
- Gray, D. F. & Nagar, P. 1985, ApJ, 298, 756
- Hatzes, A. P., Guenther, E. W., Endl, M., Cochran, W. D., Döllinger, M. P., & Bedalov, A. 2005, A&A, 437, 743
- Hekker, S., Reffert, S., Quirrenbach, A., Mitchell, D. S., Fischer, D. A., Marcy, G. W., & Butler, R. P. 2006, ArXiv Astrophysics e-prints
- Henry, G. W. 1999, PASP, 111, 845
- Henry, G. W., Baliunas, S. L., Donahue, R. A., Fekel, F. C., & Soon, W. 2000a, ApJ, 531, 415
- Henry, G. W., Fekel, F. C., & Hall, D. S. 1995, AJ, 110, 2926
- Henry, G. W., Marcy, G. W., Butler, R. P., & Vogt, S. S. 2000b, ApJ, 529, L41
- Ida, S. & Lin, D. N. C. 2005a, Progress of Theoretical Physics Supplement, 158, 68
- —. 2005b, ApJ, 626, 1045

- Johnson, J. A., Marcy, G. W., Fischer, D. A., Laughlin, G., Butler, R. P., Henry, G. W., Valenti, J. A., Ford, E. B., Vogt, S. S., & Wright, J. T. 2006, ArXiv Astrophysics e-prints
- Kornet, K., Wolf, S., & Rozyczka, M. 2006, ArXiv Astrophysics e-prints
- Laughlin, G., Bodenheimer, P., & Adams, F. C. 2004, ApJ, 612, L73
- Laws, C., Gonzalez, G., Walker, K. M., Tyagi, S., Dodsworth, J., Snider, K., & Suntzeff, N. B. 2003, AJ, 125, 2664
- Marcy, G. W., Butler, R. P., Fischer, D., Vogt, S. S., Lissauer, J. J., & Rivera, E. J. 2001, ApJ, 556, 296
- Paulson, D. B., Saar, S. H., Cochran, W. D., & Henry, G. W. 2004, AJ, 127, 1644
- Pollack, J. B., Hubickyj, O., Bodenheimer, P., Lissauer, J. J., Podolak, M., & Greenzweig, Y. 1996, Icarus, 124, 62
- Pont, F. & Eyer, L. 2004, MNRAS, 351, 487
- Queloz, D., Henry, G. W., Sivan, J. P., Baliunas, S. L., Beuzit, J. L., Donahue, R. A., Mayor, M., Naef, D., Perrier, C., & Udry, S. 2001, A&A, 379, 279
- Saar, S. H., Butler, R. P., & Marcy, G. W. 1998, ApJ, 498, L153+
- Santos, N. C., Israelian, G., & Mayor, M. 2004, A&A, 415, 1153
- Sato, B., Ando, H., Kambe, E., Takeda, Y., Izumiura, H., Masuda, S., Watanabe, E., Noguchi, K., Wada, S., Okada, N., Koyano, H., Maehara, H., Norimoto, Y., Okada, T., Shimizu, Y., Uraguchi, F., Yanagisawa, K., & Yoshida, M. 2003, ApJ, 597, L157
- Sato, B., Fischer, D. A., Henry, G. W., Laughlin, G., Butler, R. P., Marcy, G. W., Vogt,
  S. S., Bodenheimer, P., Ida, S., Toyota, E., Wolf, A., Valenti, J. A., Boyd, L. J.,
  Johnson, J. A., Wright, J. T., Ammons, M., Robinson, S., Strader, J., McCarthy, C.,
  Tah, K. L., & Minniti, D. 2005, ApJ, 633, 465
- Schrijver, C. J. & Pols, O. R. 1993, A&A, 278, 51
- Seagroves, S., Harker, J., Laughlin, G., Lacy, J., & Castellano, T. 2003, PASP, 115, 1355
- Setiawan, J., Hatzes, A. P., von der Lühe, O., Pasquini, L., Naef, D., da Silva, L., Udry, S., Queloz, D., & Girardi, L. 2003, A&A, 398, L19

- Terquem, C., Papaloizou, J. C. B., Nelson, R. P., & Lin, D. N. C. 1998, ApJ, 502, 788
- Udry, S., Mayor, M., Clausen, J. V., Freyhammer, L. M., Helt, B. E., Lovis, C., Naef, D., Olsen, E. H., Pepe, F., Queloz, D., & Santos, N. C. 2003, A&A, 407, 679
- Udry, S., Mayor, M., Naef, D., Pepe, F., Queloz, D., Santos, N. C., & Burnet, M. 2002, A&A, 390, 267
- Valenti, J. A. & Fischer, D. A. 2005, ApJS, 159, 141
- Wright, J. T. 2004, AJ, 128, 1273
- —. 2005, PASP, 117, 657
- Wright, J. T., Marcy, G. W., Butler, R. P., & Vogt, S. S. 2004, ApJS, 152, 261

This preprint was prepared with the AAS LATEX macros v5.0.

Table 1. Stellar Parameters

5.67
3.29(0.08)
0.606
G0IV
47(1.0)
+0.11 (0.05)
5980 (50)
6.1 (0.5)
3.94 (0.07)
1.28(0.1)
1.88(0.1)
0.14
-5.14
23
4.2
5.0

Table 2. Radial Velocities for HD 185269

$\begin{array}{cccccccccccccccccccccccccccccccccccc$	
13155.980     -6.5       13211.839     30.7       13522.875     -107.0       13576.840     -34.9       13619.734     -100.0       13629.661     51.7       13668.621     -21.5       13718.641     49.6       13720.587     -34.3	ertainty
13211.839     30.7       13522.875     -107.0       13576.840     -34.9       13619.734     -100.0       13629.661     51.7       13668.621     -21.5       13718.641     49.6       13720.587     -34.3	$(s^{-1})$
13522.875       -107.0         13576.840       -34.9         13619.734       -100.0         13629.661       51.7         13668.621       -21.5         13718.641       49.6         13720.587       -34.3	5.8
13576.840       -34.9         13619.734       -100.0         13629.661       51.7         13668.621       -21.5         13718.641       49.6         13720.587       -34.3	6.2
13619.734       -100.0         13629.661       51.7         13668.621       -21.5         13718.641       49.6         13720.587       -34.3	5.6
13629.661       51.7         13668.621       -21.5         13718.641       49.6         13720.587       -34.3	7.2
13668.621       -21.5         13718.641       49.6         13720.587       -34.3	5.7
13718.641 49.6 13720.587 -34.3	6.2
13720.587 -34.3	6.7
	6.3
12066 020 02 5	6.9
13866.932 $-23.5$	6.4
13867.878 11.8	4.3
13868.806 38.9	5.9
13868.996 44.3	5.6
13869.982 32.4	6.8
13879.841 -63.7	5.4
13880.912 16.0	7.1
13884.918 -50.7	5.6
13885.924 -148.0	5.5
13891.795 -66.5	6.9
13891.963 -85.7	7.0
13894.908 32.8	4.9
13895.895 44.6	5.0
13896.895 42.2	4.5
13897.908 -13.8	5.1
13898.905 -78.0	12.0
13900.929 -31.9	5.2
13901.947 $26.7$	5.7
13902.915   40.5	4.6
13903.936 29.1	5.6
13904.888 -25.6	

Table 2—Continued

JD	RV	Uncertainty
-2440000	$(m s^{-1})$	$(m s^{-1})$

Table 3. Orbital Parameters for HD  $185269\,\mathrm{b}$ 

P (d)	6.838 (0.001)
$T_p^{a}(JD)$	2453154.1 (0.18)
$T_{transit}$ (JD)	2453153.1 (0.16)
e	0.30 (0.04)
$K_1 \text{ (m s}^{-1})$	91 (4.5)
$\omega$ (deg)	173 (6.8)
$M_P \sin i \ (M_{Jup})$	0.94
a (AU)	0.077
Fit RMS (m $s^{-1}$ )	10.1
$\sqrt{\chi_ u^2}$	1.14
$N_{obs}$	30

<sup>&</sup>lt;sup>a</sup>Time of periastron passage.